



A robotic flexible endoscope with shared autonomy: a study of mockup cholecystectomy

Chengzhi Song¹ · Xin Ma² · Xianfeng Xia¹ · Philip Wai Yan Chiu^{1,2} · Charing Ching Ning Chong¹ · Zheng Li^{1,2}

Received: 10 June 2019 / Accepted: 28 October 2019
© Springer Science+Business Media, LLC, part of Springer Nature 2019

Abstract

Background Endoscope is the eye of surgeon in minimally invasive surgery (MIS). Prevailing handheld endoscopes are manually steered, which can cause endoscope-instrument fencing. Robotic endoscopes can reduce the fatigue but could not reduce collisions. Handheld endoscopes with a flexible bending tip can reduce the shaft pivoting and collisions. However, its steering is challenging. In this paper, we present a robotic flexible endoscope with auto-tracking function and compare it with the conventional rigid endoscopes.

Methods A robotic flexible endoscope (RFE) with shared autonomy is developed. The RFE could either track the instruments automatically or be controlled by a foot pedal. A mockup cholecystectomy was designed to evaluate the performance. Five surgeons were invited to perform the mockup cholecystectomy in an abdominal cavity phantom with a manual rigid endoscope (MRE), a robotic rigid endoscope (RRE), and the RFE. Space occupation, time consumption, and questionnaires based on the NASA task load index were adopted to evaluate the performances and compare the three endoscope systems. An ex vivo experiment was conducted to demonstrate the feasibility of using the RFE in a biological tissue environment.

Results All surgeons completed the mockup cholecystectomy with the RFE independently. Failure occurred in the cases involving the RRE and the MRE. Inside the body cavity, the space occupied when using the RFE is 17.28% and 23.95% ($p < 0.05$) of that when using the MRE and the RRE, respectively. Outside the body cavity, the space occupied when using the RFE is 14.60% and 15.53% ($p < 0.05$) of that by using MRE and RRE. Time consumed in the operations with MRE, RRE, and RFE are 28.3 s, 93.2 s and 34.8 s, respectively. Questionnaires reveal that the performance of the RFE is the best among the three endoscope systems.

Conclusions The RFE provides a wider field of view (FOV) and occupies less space than rigid endoscopes.

Keywords Minimally invasive surgery · Cholecystectomy · Robotic flexible endoscope · Shared autonomy

Chengzhi Song, Xin Ma and Zheng Li contributed equally to this work.

✉ Zheng Li
lizheng@cuhk.edu.hk
Philip Wai Yan Chiu
philipchiu@surgery.cuhk.edu.hk
Charing Ching Ning Chong
chongcn@surgery.cuhk.edu.hk

¹ Department of Surgery, The Chinese University of Hong Kong, Shatin, N.T., Hong Kong SAR

² Chow Yuk Ho Technology Centre for Innovative Medicine, The Chinese University of Hong Kong, Shatin, N.T., Hong Kong SAR

Minimally invasive surgery (MIS) has revolutionized the traditional surgery with its advantages of less suffering, less chance of postoperative infection, and quicker postoperative recovery [1]. In MIS, the endoscope is inserted through a trocar and provides surgeons with the vision inside body cavity [2]. Nowadays, prevailing endoscopes are rigid and slender in structure. Challenges of using these endoscopes are: (1) making the endoscope assistants suffer from fatigue; (2) highly dependent on smooth cooperation between the endoscope assistant and the surgeons [3]; (3) demanding large motion space when pivoting the rigid structure endoscope [4]; and (4) limited FOV. To address these challenges, several solutions are developed.

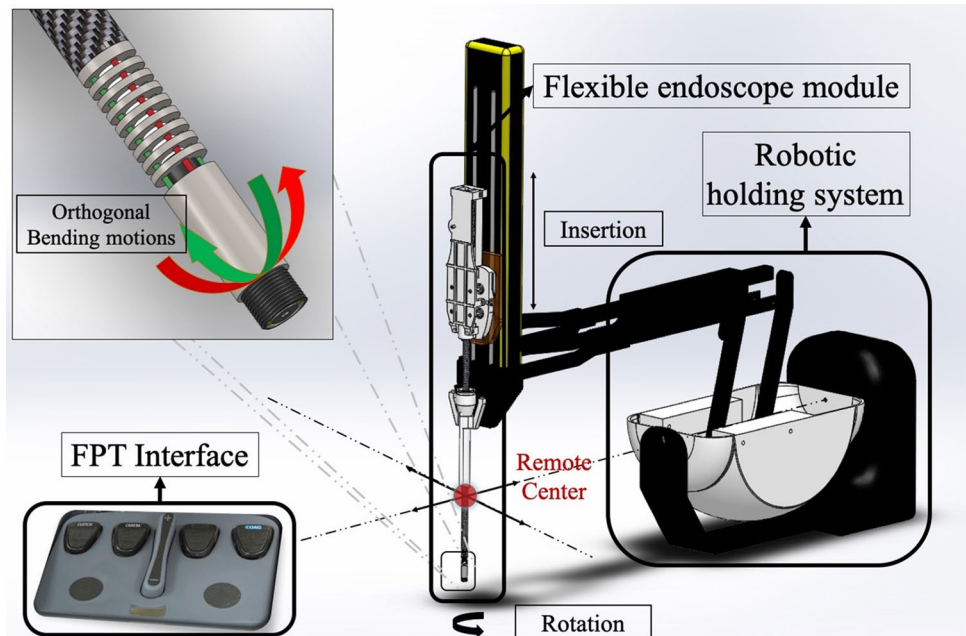
Many robotic endoscopes holding systems have been developed to avoid the fatigue of surgeons, reduce human errors (such as hands trembling) when manipulating the

endoscope, and smooth the operations. Notable systems are the 4-DOF automated endoscope system for optimal positioning (AESOP) [5], the laparoscopic assistant robot system [6], the EndoAssist [7], the vision control endoscopy [8], the lightweight synthetic muscle actuator-based robotic technology [9], low-cost RoboLens [10], and the SOLOASSIST [11], etc. However, these systems are based on rigid structure which leads to a lack of dexterity and limited FOV as reported in reference [12]. A large motion space of the robotic endoscopes holding systems is needed when operating the rigid robotic endoscopes [13–16]. Endoscopes with bendable distal section such as the manually controlled EndoEye Flex [17] and Cardioscope [18] are proposed. However, driving endoscopes with flexible structure entails a long learning curve. One promising solution is integrating the flexible structure based endoscope with the robotic endoscope holding system. In reference [19], attempts are made to motorize the bending of the flexible tip with a manually controlled shaft. More recently, a head-mounted Gyro and a foot pedal are used as human–robot interfaces to control the motion of a flexible endoscope [20]. However, these two systems mainly rely on the manual view control. In this paper, the RFE with shared autonomy, i.e., automatic view tracking combined with user control override, is proposed.

Materials and methods

This work does not contain animal/human study. No IRB (institutional review board) approval is required.

Fig. 1 The CAD model of the RFE system: a flexible endoscope module, a robotic holding system, and a foot pedal interface for shared control



The robotic flexible endoscope

As shown in Fig. 1, the RFE is mainly composed of three parts: a flexible endoscope module, a robotic holding system (Patient Side Manipulator from dVRK [21]), and a user interface (FPT).

- 1) The flexible endoscope module, as shown in Fig. 2, consists of four parts: a flexible wrist, a camera module, a carbon-fiber shaft, and a self-designed mounting backend. The design of the flexible wrist is based on the continuum mechanism [22, 23]. It has eight disks and two adapters, as shown in Fig. 3A. The length and the outer diameter of the flexible wrist

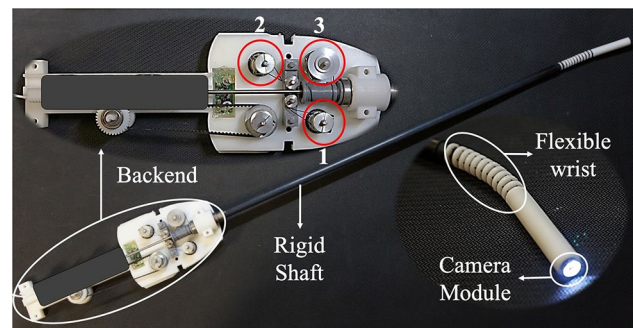


Fig. 2 Prototype of the flexible endoscope module. It consists of four parts: a camera module, a flexible wrist, a carbon-fiber shaft, and a mounting backend. This module provides three motions: one rolling motion and two orthogonal bending motions

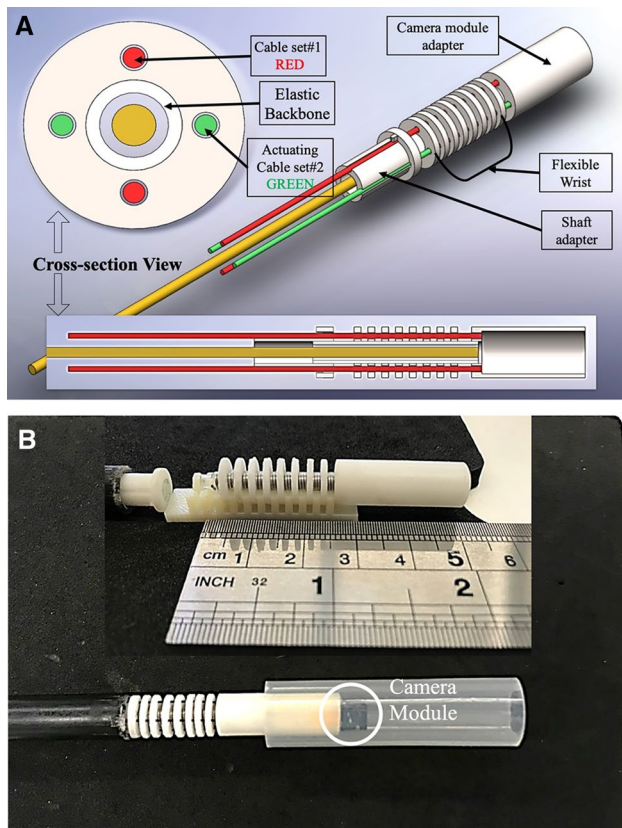


Fig. 3 Design and the dimension of the flexible wrist. **A** The design of the flexible wrist is based on the continuum mechanism which is driven by four cables. The flexible wrist consists of eight disks. On each disk, there are four holes symmetrically distributed to pilot the cables. The flexible wrist can provide two orthogonal bending motions. **B** The prototype of the flexible wrist. The thickness of each disk is 1 mm. And the eight disks are equally spaced with a distance of 2 mm, which makes the total length of flexible wrist 26 mm. Vertebrae have an outer diameter of 7.5 mm, with 4 pilot holes that have a diameter of 1 mm. The camera module is installed at the end of the flexible wrist by a 25 mm long adapter

are 26 mm and 7.5 mm, respectively. As shown in Fig. 3B, the camera module is a mini camera (MD-V21106L-128, MISUMI ELECTRONIC CORP) which has a resolution of 640×480 pixel and runs at thirty frames per second. The length of the carbon-fiber shaft is 416 mm. The self-designed mounting backend is the interface for integrating with the robotic holding system.

- 2) Robotic holding system: the patient side manipulator (PSM) from the dVRK is adopted as the robotic holding system which provides yaw, pitch, and in/out insertion motions for the flexible endoscope module.

- 3) Control interface: the foot pedal tray (FPT) is utilized as the interface for surgeons. As shown in Fig. 4, five buttons on the foot pedal tray are activated to receive the commands from operating surgeons.

Shared autonomy control for the RFE

In this paper, a vision command combined (VCC) interface is proposed to realize the shared autonomy of the RFE. The ‘vision’ refers to the vision-based auto-tracking function, and the ‘command’ means the commands obtained from the surgeons through an interface (FPT) [24]. With the proposed VCC interface, surgeons can turn ON/OFF the auto-tracking function, rotate the endoscope axially, and zoom IN/OUT the endoscope through a foot pedal tray (FPT), as shown in Fig. 4.

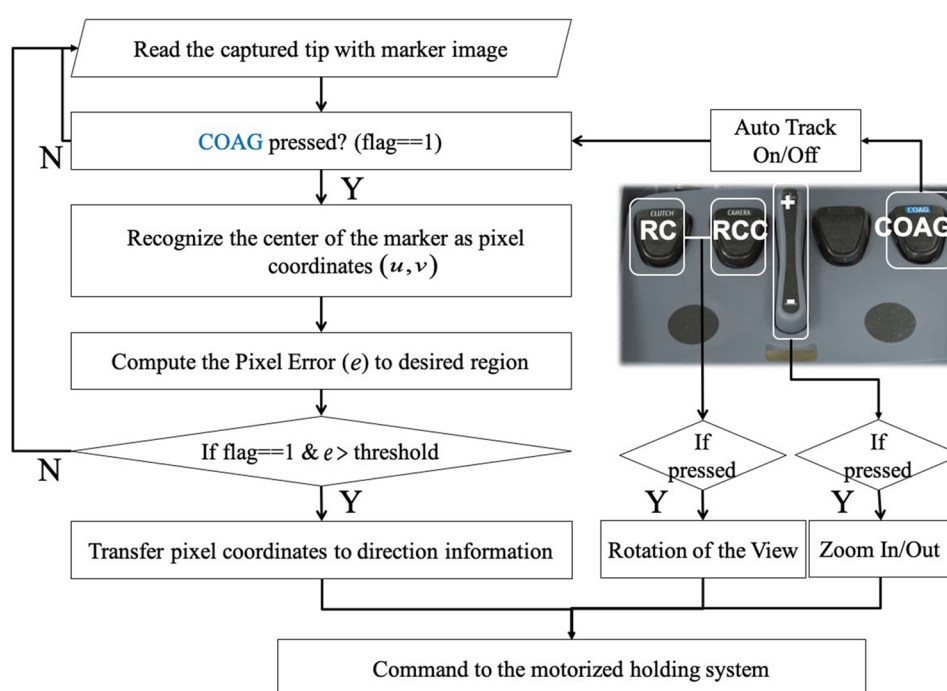
Auto-tracking is realized with visual servoing [24, 25]. As illustrated by the flow chart in Fig. 4, once the button ‘COAG’ is pressed, the RFE starts auto-tracking. During the auto-tracking, the images obtained by the RFE are collected and processed to detect blue markers. If the RFE successfully detects a marker, the program proceeds to extract the coordinate (position in the images) of the detected blue marker. The controller will then minimize the error between the extracted coordinate and the center of the images. If two or more markers are detected at the same time, the geometrical center of the markers will be tracked.

Study design: mockup cholecystectomy

In this work, mockup cholecystectomy is designed to compare the performances of the three endoscope systems which are based on the same hardware. By disabling the bending motions, the RFE system is able to simulate one control group, i.e., the robotic rigid endoscope (RRE) system. By further disabling all the motions, the system can be adopted as the other control group, i.e., the manually controlled rigid endoscope (MRE) system.

Apart from time consumption, the occupied space is another important indicator of performance of the RFE to be evaluated. In this paper, the occupied space refers to the spatial volume occupied by the systems’ hardware. And the occupied space can be computed as follows: (1) all joint positions are recorded by a computer at 100 Hz frequency during the whole operation; (2) kinematic model is used to describe the configuration of the three endoscope systems respectively with the recorded joint

Fig. 4 Shared autonomy control for the RFE. The corresponding functions of the five buttons are as follows: (1) 'RC' button: when pressed, the RFE rotates clockwise and axially. (2) 'RCC' button: when pressed, the RFE rotates counterclockwise and axially. (3) '+' button: zoom in. (4) '-' button: zoom out. (5) 'COAG' button: when pressed, turns on the auto-tracking. The algorithm for auto-tracking is shown within the left flowchart



positions; (3) the occupied space is determined by the envelope of all the configurations in the tracking process.

The setup for the mockup cholecystectomy is shown in Fig. 5. A silicon liver model is placed inside the phantom, and the dark green balloon is used to simulate the gallbladder. The green straw is used to simulate the cystic duct, as shown in Fig. 6. Three laparoscopic instruments are used in this study: a pair of scissors, a grasper, and a retractor. Blue markers were attached on the tip of each instrument.

The mockup cholecystectomy includes six steps:

- 1) Insert a grasper until it appears on the image display;
- 2) Guide the endoscope (automatic/manual) with the grasper to the 'gallbladder' with a satisfactory view;
- 3) Insert the retractor until it appears on the image display;
- 4) Lift the 'gallbladder' and liver with the retractor until the cystic duct is exposed;
- 5) Insert the scissors and cut the cystic duct (green straw);
- 6) Retrieve specimen (the dissected 'gallbladder') with the grasper.

Five skilled surgeons participated in this study. Each surgeon was asked to perform the mockup cholecystectomy three times by using the three different endoscope systems (MRE, RRE, and RFE) through the conventional port (incision #1, as shown in Fig. 5), respectively. In addition, it is expected that there is a higher chance of

instrument-endoscope fencing at incision #1 of the umbilicus area, which can show the differences between the three endoscope systems clearly. All the operations were repeated in an unconventional location (incision #2 of the epigastrium region, as shown in Fig. 5) where there is a lower chance of fencing. During the study, the operating time and endoscope motions were recorded at a frequency of 100 Hz for quantitative analysis.

Cholecystectomy: ex vivo experiment

The ex vivo cholecystectomy with porcine liver and gallbladder was conducted by another skilled surgeon. The objective of this experiment is to demonstrate the feasibility of the RFE to work in a biological tissue environment, as shown in Fig. 6. The surgeon controlled the RFE with the shared autonomy method. The porcine liver and gallbladder were placed on a steel plate inside the phantom.

Results

The FOV

The maximum pitch angle of the robotic holding system and the maximum yaw angle are 60° and 90°, respectively. The motion range of insertion is from 0 to 240 cm. The rotation range of the rolling shaft is from -180° to

Fig. 5 System setup for the mockup cholecystectomy and the simulation environment. Incision #1 (umbilicus area) on the phantom is the conventional location for endoscope insertion in cholecystectomy. Incision #2 (epigastrium) on the phantom is chosen as the location to repeat the operation. **A** System setup for the mockup cholecystectomy. An optical bench is utilized to place the RFE system. The laparoscopic phantom is set on a medical trolley. The monitors are placed near the system for streaming. The PC is placed on the bottom layer of the trolley. **B** Setup of the mockup cholecystectomy within the phantom. A 1:1 liver model, a dark green balloon (gallbladder), and a green straw (cystic duct) are set inside the phantom to simulate the cholecystectomy (Color figure online)

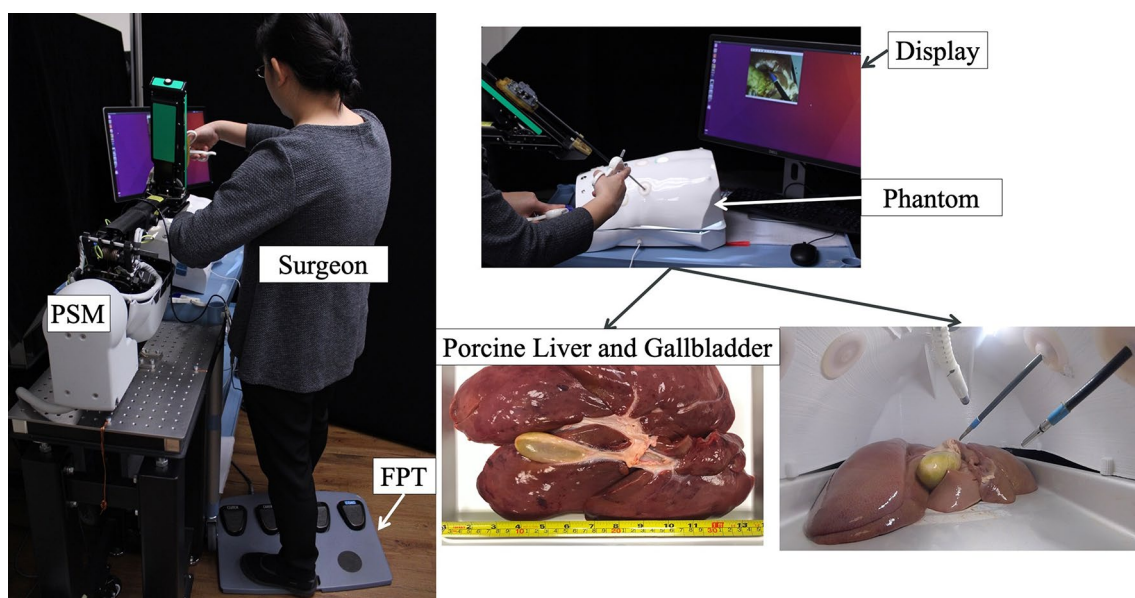
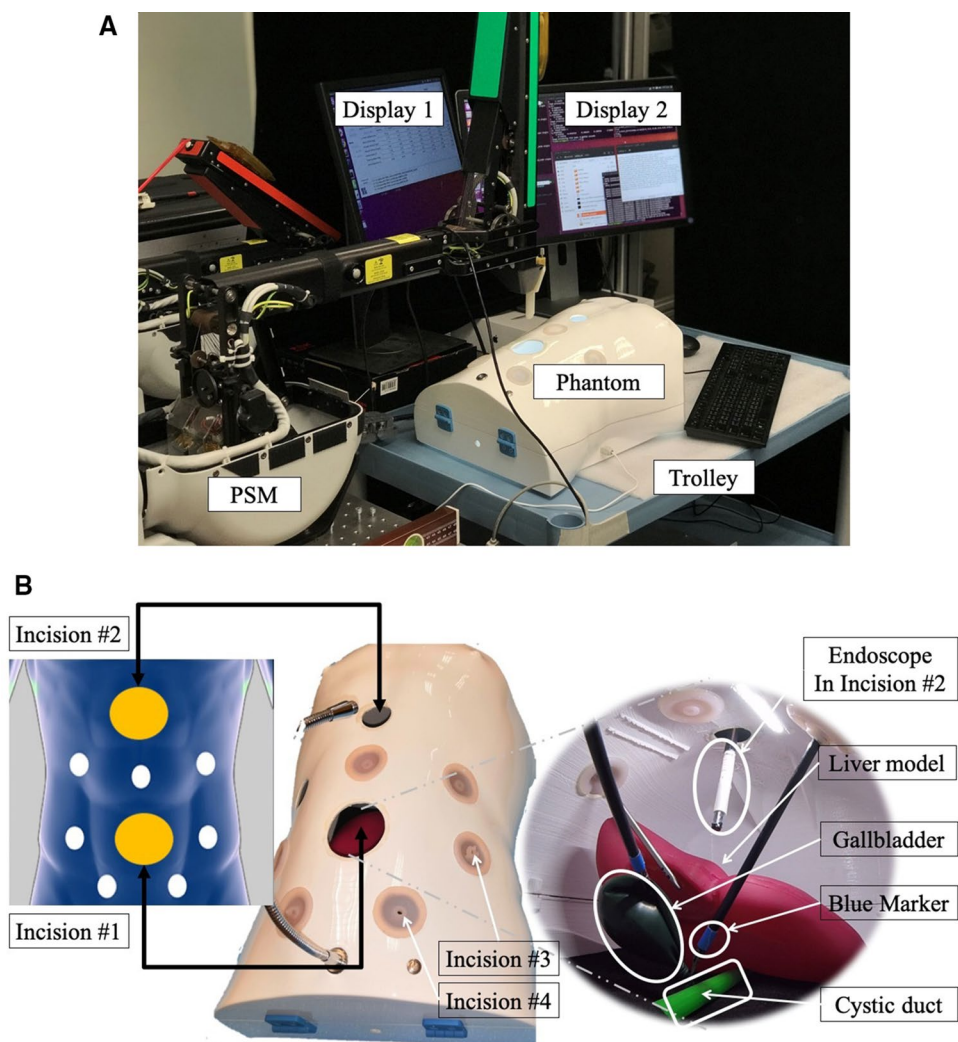


Fig. 6 Ex vivo cholecystectomy experiment with porcine liver and gallbladder

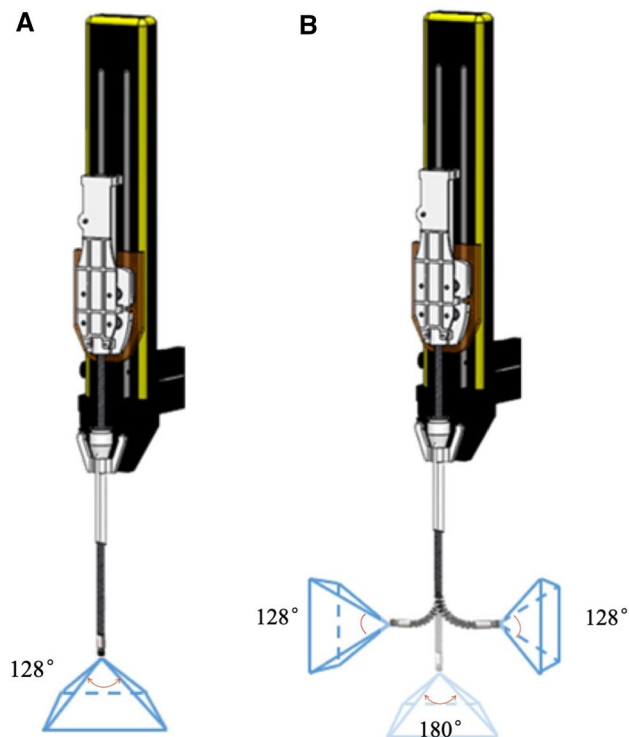


Fig. 7 The illustration of the FOV of rigid and flexible endoscope systems with the same camera and the same robotic holding system (PSM). **A** The FOV of the rigid endoscope at one configuration, which is only determined by the camera's FOV (128°). **B** The FOV of the RFE is enlarged from 128° to 308° due to the $\pm 90^\circ$ bending motion provided by the flexible wrist

180°. The maximum bending angle of the flexible wrist could reach $\pm 90^\circ$. Compared with a rigid endoscope, the proposed RFE can expand the FOV from 128° to 308° without moving the robotic holding system as illustrated in Fig. 7. With a larger FOV, the RFE has more options of incision locations (taking incision #2 in the mockup cholecystectomy as an example).

Analysis of occupied space

A total of thirty operations were conducted by five surgeons. The first fifteen operations were conducted with endoscopes inserted at the umbilicus area (incision #1). At this port, subjects were all able to finish the operations by using the RRE and the RFE without any help from endoscope assistants. In the case of the MRE, an endoscope assistant was needed to manipulate the endoscope under the instruction of the subject. In the other fifteen operations, endoscopes were inserted at the epigastrium

Fig. 8 The visualized reproduction of sampled trajectories conducted by one participant using the three endoscope systems respectively. Blue lines illustrate the trajectory of the robotic holding system. Red lines are the trajectories of rigid endoscope module of the RRE/MRE and the rolling shaft of the RFE. Green curves represent the trajectories by the flexible wrist of the flexible endoscope module. **A** Trajectory of the MRE in incision #1. **B** Trajectory of the RRE in incision #1. **C** Trajectory of the RFE in incision #1. **D** Trajectory of the MRE in incision #2. **E** Trajectory of the RRE in incision #2. **F** Trajectory of the RFE in incision #2 (Color figure online)

area (incision #2). When using the MRE or the RRE, another assistant was needed to help to lift the 'liver' to expose the gallbladder. In cases with the RFE, no assistant was needed. Incision #2 was set further away from the locations for the operating instruments compared with incision #1. Therefore, there would be more space for the operation and lower possibility of collision with the instruments.

By recording the joint values of the robotic holding system and applying the kinematic model, the motion sequences of the endoscopes during the operations could be drawn as in Fig. 8. Then the occupied space can be calculated. The results are summarized in Tables 1 and 2.

The statistic results of the occupied space with different endoscope systems are shown in Fig. 9. The smallest occupied space was registered by RFE with a statistically significant difference, as compared with the MRE ($p < 0.05$) and RRE ($p < 0.05$). However, in each operation, the desired view and position of the endoscope for each operating surgeon could be different. Therefore, the ratio of the occupied space by using the flexible endoscope to that of rigid endoscope varied in the range of 8.28–33.97%, as listed in Tables 1 and 2.

More specifically, in incision #1, the ratios of occupied space by using the RFE to that by using the MRE and the RRE are 20.11–25.69% inside the body cavity (phantom). The ratios of occupied space outside the phantom by using the RFE are reduced to 14.28% and 14.96% to that by using the MRE and RRE, respectively. The corresponding ratios with respect to incision #2 are 14.44% and 22.21%, inside the phantom; 14.92%, and 16.10%, outside the phantom, respectively.

The average ratios of occupied space inside the phantom by using the RFE to the occupied space by using the MRE and the RRE are 17.28% and 23.95%, respectively; the average space occupied outside the phantom by the proposed RFE are 14.60% and 15.53% to that by using the MRE and RRE, respectively. Therefore, it could be concluded that the proposed RFE could significantly reduce the space occupation compared with rigid endoscopes,

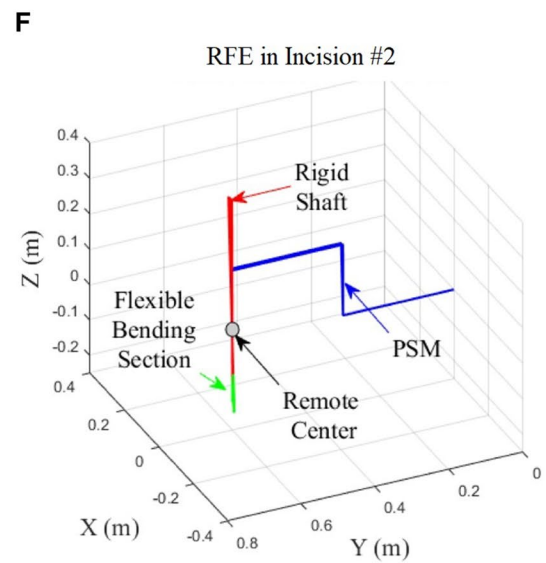
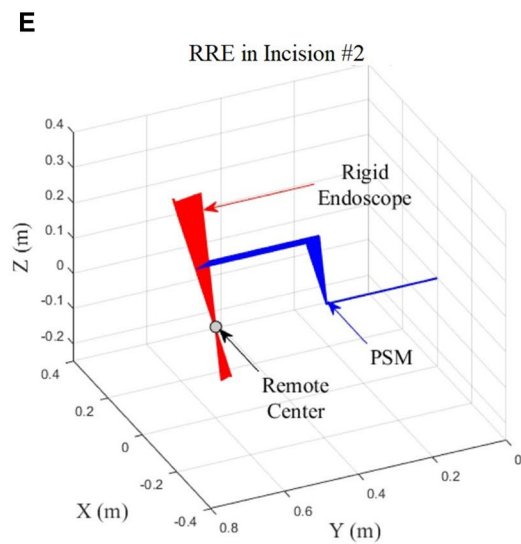
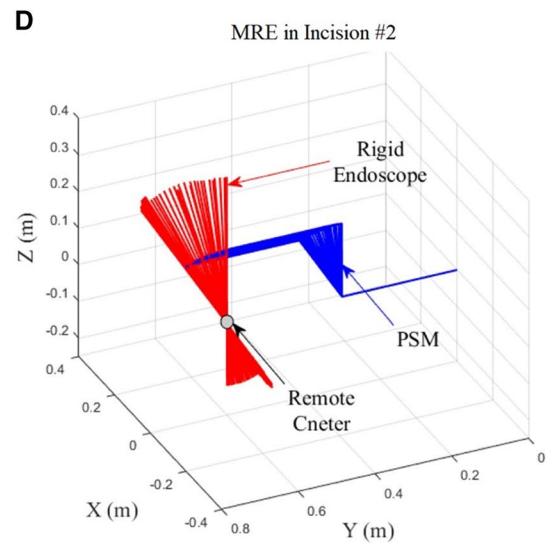
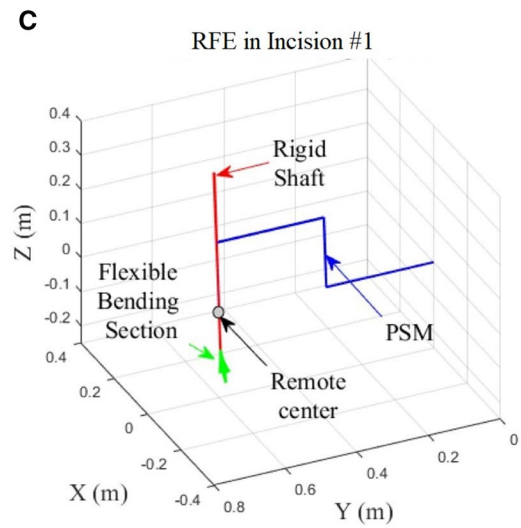
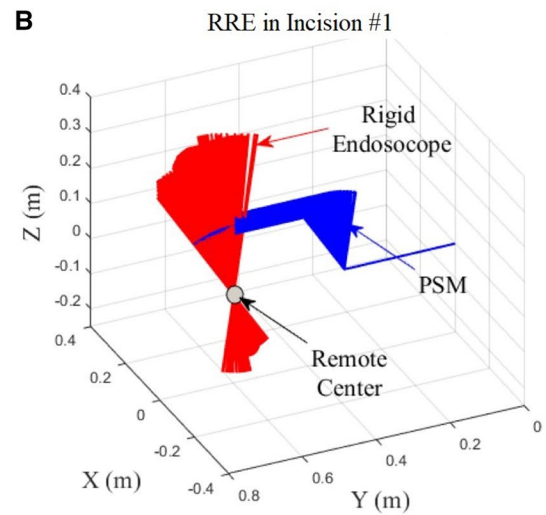
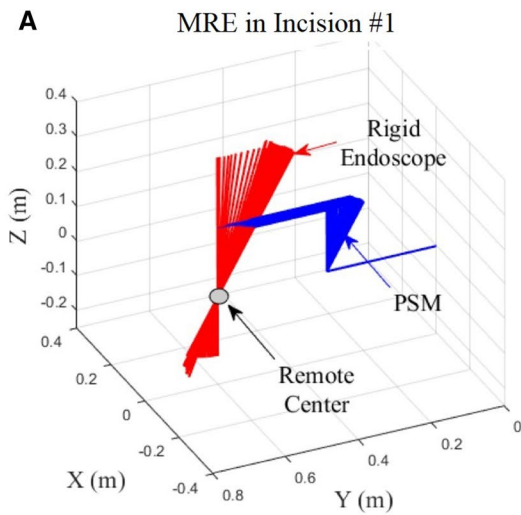


Table 1 The occupied space of each operation (incision #1)

	MRE occupied space (liter)		RRE occupied space (liter)		RFE occupied space (liter)		RFE/MRE (%)		RFE/RRE (%)	
	Inside	Outside	Inside	Outside	Inside	Outside	Inside (%)	Outside (%)	Inside (%)	Outside (%)
1	2.069	24.279	1.678	25.922	0.390	2.811	18.85	11.58	23.24	10.84
2	0.595	14.057	0.589	13.717	0.126	2.445	21.18	17.39	21.39	17.82
3	0.645	15.487	0.561	13.090	0.156	1.906	24.19	12.31	27.81	14.56
4	0.872	16.814	0.636	16.349	0.148	3.000	16.97	17.84	23.27	18.35
5	0.692	15.810	0.409	14.700	0.134	1.945	19.36	12.30	32.76	13.23
Stat.	0.975 ± 0.62	17.289 ± 4.030	0.775 ± 0.512	16.755 ± 5.270	0.191 ± 0.112	2.421 ± 0.495	20.11	14.28	25.69	14.96

Table 2 The occupied space of each operation (incision #2)

	MRE occupied space (liter)		RRE occupied space (liter)		RFE occupied space (liter)		RFE/MRE (%)		RFE/RRE (%)	
	Inside	Outside	Inside	Outside	Inside	Outside	Inside (%)	Outside (%)	Inside (%)	Outside (%)
1	1.980	23.252	0.841	19.345	0.164	3.241	8.28	13.94	19.50	16.75
2	0.502	10.722	0.365	10.496	0.124	1.848	24.70	17.24	33.97	17.61
3	0.621	11.487	0.401	10.648	0.088	1.608	14.17	14.00	21.95	15.10
4	0.818	14.604	0.606	14.428	0.117	2.575	14.30	17.63	19.31	17.85
5	0.877	15.252	0.575	13.636	0.094	1.801	10.72	11.81	16.35	13.21
Stat.	0.960 ± 0.590	15.063 ± 4.973	0.536 ± 0.265	13.711 ± 3.605	0.117 ± 0.03	2.215 ± 0.681	14.44	14.92	22.21	16.10

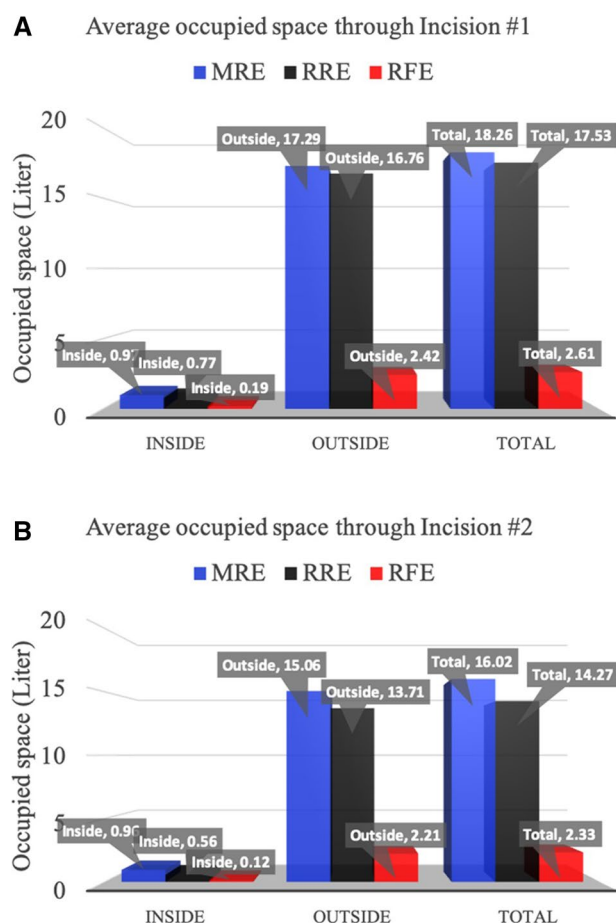


Fig. 9 Comparison of the occupied motion space by using three endoscope systems. **A** Average occupied space through Incision #1; **B** Average occupied space through Incision #2

including RRE and MRE. The reduced space occupation could provide more space for the surgeons to operate and reduce the chance of collisions with instruments.

Operating time

The operating time for cholecystectomy with different endoscope systems is shown in Fig. 10. Through incision #1, it takes 28.3 s, 93.2 s, and 34.8 s on average to perform cholecystectomy with the MRE, the RRE, and the RFE, respectively. Through incision #2, it takes 31.6 s, 67.8 s, and 45.2 s for the MRE, the RRE, and the RFE, respectively to complete the procedure. Among all the cases, the shortest overall operating time is 24.5 s. It is registered in a case with the MRE, in which two assistants were involved (one for steering the MRE and the other for retracting the liver). The RRE took the longest time and was a lot longer than that with the MRE and the RFE. The operation time with MRE was a little shorter than that with RFE. The reason is that the moving speed of the robot was

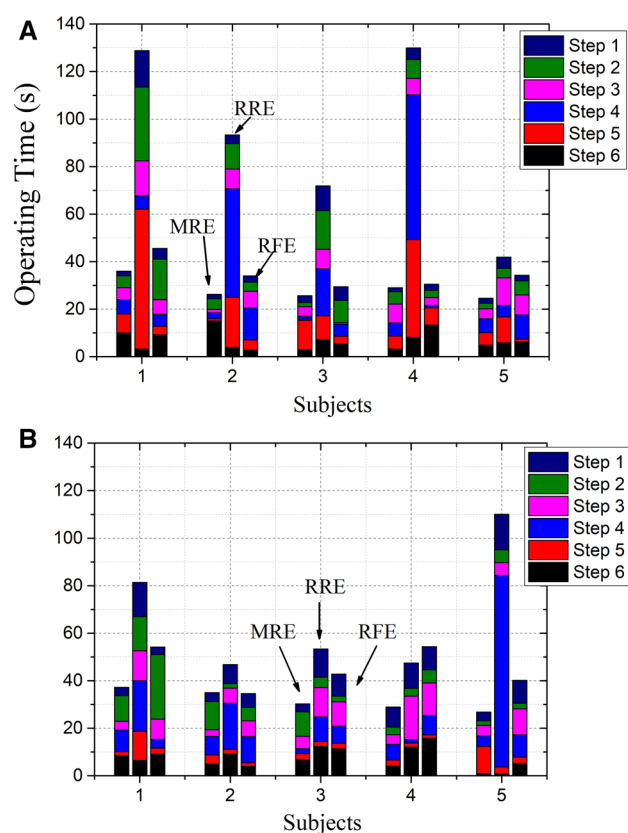


Fig. 10 Charts for operating time. The horizontal axis represents the subjects 1–5. Vertical axis stands for the time cost chart for each step with the endoscopes. For each subject, three bars represent time cost with the MRE, the RRE, and the RFE, respectively. The total time cost is the sum of the time cost for each step. The dark blue box represents the time cost to manipulate the instruments in the view of the endoscope. Green box, pink box, blue box, red box, and black box represent time cost for task 2–6 sequentially. **A** Incision #1. **B** Incision #2 (Color figure online)

restricted for safety reasons. The operating time by using the RFE was much shorter than the operating time with the RRE. The reason might be that the surgeons need to take care of the fencing with the endoscope-holding robot due to the largest occupied space of the rigid endoscope. In addition, the motion of the RRE is larger, which also leads to a long operating time.

In the case of incision #1, step 2 (guiding the endoscopes) and step 5 (inserting the scissors and cutting the cystic duct) contribute a lot to subject the one with RRE. This subject shows concern of collision with instruments during operating the rigid endoscope alone which slows down the procedure. Step 4 (retracting the gallbladder and exposing the cystic duct) and step 5 play a major role in time consumption for subjects two, three, and four during operations with the RRE. The feedback of the subjects reveals that they all have concern on the possible collisions with the robot arm during the operation with the RRE.

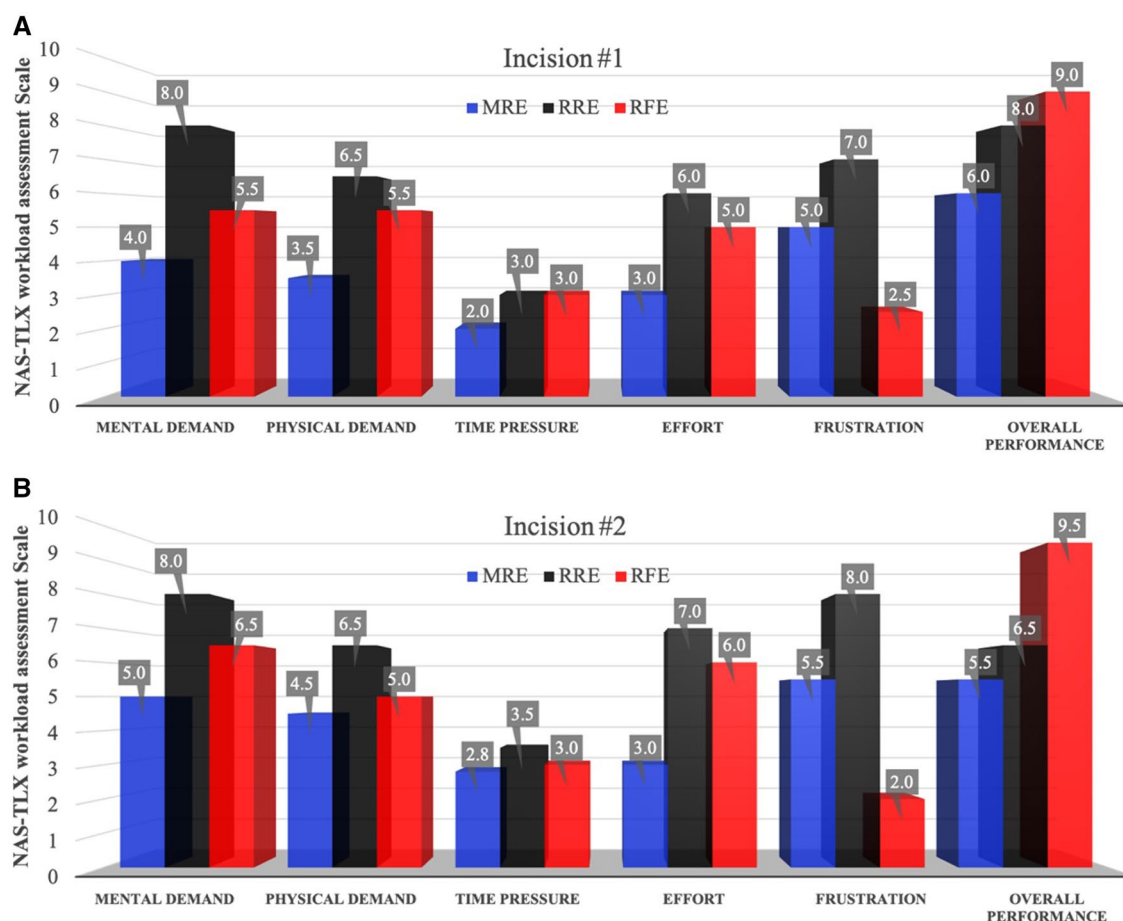


Fig. 11 Average scales for each dimension of the NASA-TLX, including mental demand, physical demand, time pressure, overall performance evaluation, Frustration, and Effort. The blue bars are the information for MRE. The black bars are the information for RRE

and the red bars are the information for the RFE. **A** Assessment for three endoscope systems through incision #1. **B** Assessment for three endoscope systems through incision #2 (Color figure online)

In the case of incision #2, the time cost with the RRE decreased except for subject five. All subjects showed fewer concerns of fencing with instruments due to the further distance of the endoscope. While for subject five, step 4 took far longer than that of others. This was because of the suboptimal retraction from the helper that led to limited exposure to the cystic duct.

Questionnaire

In this study, a questionnaire was designed based on the NASA task load index (TLX) to evaluate the user experience with the endoscopes [26]. The NASA-TLX was initially used as a tool for subjective evaluation of individual's workload in flight simulation, automated and manual control, etc. [27]. Nowadays, it has also been used for the assessment of user experience with medical robots/devices [28]. In the questionnaire, the subjects were required to rate the 'Mental Demand', 'Physical

Demand', 'Time Pressure', 'Effort', 'Frustration', and 'Overall Performance' from 0 to 10. In all these items, lower marks reflect better evaluation, except for the 'Overall Performance'.

The results are shown in Fig. 11. In all the operations, the MRE scored the lowest in terms of 'Mental Demand', 'Physical Demand', 'Time Pressure', and 'Effort'. This is partially attributed to the fact that an additional endoscope assistant is involved and the subjects are more familiar with it. In these items, the RFE scored lower than the RRE. In terms of 'Frustration', the RFE scored the lowest. In terms of 'Overall Performance', the RFE scored the highest. The possible reason is that the RFE could track the instruments with a wider FOV. In addition, it is found that among all the endoscope systems, the score with incision #1 was over than that with incision #2 in terms of 'Mental Demand', 'Physical Demand', 'Time Pressure', and 'Effort'. For the 'Frustration', the score for RFE was lower with incision #2. In terms of

'Performance', the MRE and the RRE showed higher score with incision #1, while the RFE showed higher score with incision #2.

Discussion

The proposed RFE provides a larger FOV inside the body cavity compared with rigid endoscopes (the MRE and the RRE). With the enlarged FOV, the choice of port for flexible endoscope systems could be more flexible. This allows the surgeons choosing ports that are far away from the instrument ports during the operation.

According to the comparison of the occupied space by using the three endoscope systems, the occupied space of the MRE was the largest. The RRE and RFE are automatically controlled with visual guidance, which provides a more precise vision control. The drastic reduction of the occupied motion space with the RFE has two reasons: the first one is that the flexible structure of the proposed RFE allows for distal viewing angle control, and the second one is that the joints' motions were further reduced by the control algorithm, in which weight factors were used to control the joint motion.

The operating time with the RFE is much shorter than the operating time with RRE. That might be due to the subjects' concerns of the collision when they were operating with the rigid endoscopes. On the other hand, since the RRE does not allow distal view control, it requires larger motion that costs more time. The least time cost of performing cholecystectomy is by using the MRE. It could be explained by that the speed of the robot was restricted to eliminate the safety concerns from the participants since they are not used to operating alongside the robot. On the other hand, the speed of manually steering the endoscope was unrestricted. Another possible reason is that the surgeons are more confident when working along with the assistant. This also helps to speed up the operation.

The NASA-TLX assessment showed that subjects consider the RFE better than the RRE in terms of all dimensions. This might be because that the RFE was easier to control with the VCC method for subjects, and it provides smooth tracking with smaller occupied space. Although operations with the RFE demand more than those with the MRE in terms of 'Mental Demand', 'Physical Demand', 'Time Pressure', and 'Effort' dimension, the RFE still outperformed the MRE with respect to the frustration and performance. Decreased frustration level could be explained by the reduction of the motion space, which helps to reduce the surgeons' concerns of fencing during operations.

According to the assessment of operations with endoscopes inserted through different ports, incision #1 was

better for both the MRE and RRE. When the MRE and the RRE were inserted through incision #1, a better view than that with incision #2 was presented. In addition, the manipulation of the endoscopes was more intuitive. When inserted through incision #2, the assistant's support was more frequent. In terms of the RFE, the use of incision #1 and incision #2 showed similar performance, including space occupation and operation time. From the NASA-TLX, the overall performance when using incision #2 is a little better. One of the possible reasons is that the endoscope was placed further away from the instruments, thus allowing more space for operation. This also shows that with the wider FOV and enhanced dexterity inside the body cavity, the flexible endoscope provided more options for the port placement without sacrificing the performance.

It should be pointed out that the presented RFE is only a prototype. To be used in clinical settings, much refinement remains to be done. For example, the image quality needs to be advanced to higher definition (HD), or even stereovision. The dimension of the shaft is 8 mm and could be further reduced to 5 mm. Lens cleaning and defogging needs to be considered to reduce the retraction during operation. Last, sterilization needs to be considered.

Acknowledgements This work is supported by the Hong Kong Research Grants Council (RGC) with Project Numbers (14212316, 14207017 and 24204818) and CUHK-SJTU Joint Research Collaboration Fund.

Compliance with ethical standards

Disclosures Philip Waiyan Chiu serves as the scientific advisory board member of Aptom Co Ltd and scientific advisory board member of EndoMASTER Pte Ltd. Chengzhi SONG, Xin MA, Xianfeng XIA, Charing CN CHONG, and Zheng LI have no conflict of interest or financial ties to disclose.

References

1. Fuchs KH (2002) Minimally invasive surgery. *Endoscopy* 34(02):154–159
2. Vitiello V, Lee SL, Cundy TP, Yang GZ (2012) Emerging robotic platforms for minimally invasive surgery. *IEEE Rev Biomed Eng* 6:111–126
3. Dakin GF, Gagner M (2003) Comparison of laparoscopic skills performance between standard instruments and two surgical robotic systems. *Surg Endosc* 17:574–579
4. Freschi C, Ferrari V, Melfi F, Ferrari M, Mosca F, Cuschieri A (2013) Technical review of the da Vinci surgical telemanipulator. *Med Robot Comput Assist Surg* 9:396–406
5. Wang Y (1996) Automated endoscope system for optimal positioning. *CIM-INT MANUF* 12(4):372

6. Taylor RH, Funda J, Eldridge B, Gomory S, Gruben K, LaRose D, Talamini M, Kavoussi L, Anderson J (1995) A telerobotic assistant for laparoscopic surgery. *IEEE Eng Med Biol Mag* 14(3):279–288
7. Gilbert JM (2009) The EndoAssist™ robotic camera holder as an aid to the introduction of laparoscopic colorectal surgery. *Ann R Coll Surg Engl* 91(5):389–393
8. Voros S, Haber GP, Menudet JF, Long JA, Cinquin P (2010) ViKY robotic scope holder: initial clinical experience and preliminary results using instrument tracking. *IEEE-ASME T MECH* 15(6):879–886
9. Taniguchi K, Nishikawa A, Sekimoto M, Yasui M, Takiguchi S, Seki Y, Monden M, Miyazaki F (2006) Design of a novel wearable laparoscope manipulator: SMART (Synthetic Muscle Actuator based Robotic Technology). *Int J Comput Assist Radiol Surg* 1:213
10. Mirbagheri A, Farahmand F, Meghdari A, Karimian F (2011) Design and development of an effective low-cost robotic camera-man for laparoscopic surgery: RoboLens. *Sci Iran* 18(1):105–114
11. Kristin J, Geiger R, Kraus P, Klennzer T (2015) Assessment of the endoscopic range of motion for head and neck surgery using the SOLOASSIST endoscope holder. *Int J Med Robot* 11(4):418–423
12. Wijsman PJ, Broeders IA, Brenkman HJ, Szold A, Forgione A, Schreuder HW, Consten EC, Draaisma WA, Verheijen PM, Ruurda JP, Kaufman Y (2018) First experience with THE AUTO-LAP™ SYSTEM: an image-based robotic camera steering device. *Surg Endosc* 32(5):2560–2566
13. Mettler L, Ibrahim M, Jonat W (1998) One year of experience working with the aid of a robotic assistant (the voice-controlled optic holder AESOP) in gynecological endoscopic surgery. *Hum Reprod (Oxford, England)* 13(10):2748–2750
14. Arezzo A, Ulmer F, Weiss O, Schurr M, Hamad M, Buess GF (2000) Experimental trial on solo surgery for minimally invasive therapy. *Surg Endosc* 14(10):955–959
15. Holländer SW, Klingen HJ, Fritz M, Djalali P, Birk D (2014) Robotic camera assistance and its benefit in 1033 traditional laparoscopic procedures: prospective clinical trial using a joystick-guided camera holder. *Surg Technol Int* 25:19–23
16. Ozaki R, Kumakiri J, Kikuchi I, Kitade M, Matsuoka S, Jinushi M, Kono A, Takeda S (2011) Beneficial use of ENDOCAMEL-EON a novel optical devise for single port laparoscopic surgery for large ovarian cyst. *J Minim Invasive Gynecol* 18(6):S113
17. Ronald C, Rami L, Marc S, Brett C, Marcos M, Todd W (2014) Improving precision and accuracy in laparoscopy using the ENDOEYE FLEX 3D articulating videoscope. <https://www.generalsurgerynews.com/Monographs-Whitepapers/Article/04-14/Improving-Precision-and-Accuracy-in-Laparoscopy-Using-the-ENDOEYE-FLEX-3D-Articulating-Videoscope/27350>. Accessed 22 Mar 2014
18. Li Z, Oo MZ, Nalam V, Thang VD, Ren H, Kofidis T, Yu H (2016) Design of a novel flexible endoscope—cardioscope. *J Mech Robot* 8(5):051014
19. Ko SY, Kim J, Lee WJ, Kwon DS (2007) Compact laparoscopic assistant robot using a bending mechanism. *ADV Robot* 21(5–6):689–709
20. Luo RC, Wang J, Chang CK, Perng YW (2014, August) Surgeon's third hand: an assistive robot endoscopic system with intuitive maneuverability for laparoscopic surgery. In: 5th Proceedings of the IEEE RAS EMBS International Conference Biomedical Robotics and Biomechatronics, pp 138–143
21. Kazanzides P, Chen Z, Deguet A, Fischer GS, Taylor RH, DiMaio SP (2014, May) An open-source research kit for the da Vinci® Surgical System. In: 2014 IEEE International Conference on Robotics and Automation, pp 6434–6439
22. Li Z, Du R (2013) Design and analysis of a bio-inspired wire-driven multi-section flexible robot. *IJARS* 10(4):209
23. Li Z, Ren H, Chiu PWY, Du R, Yu H (2016) A novel constrained wire-driven flexible mechanism and its kinematic analysis. *MMT* 95:59–75
24. Ma X, Song C, Chiu WYP, Li Z (2019) Autonomous flexible endoscope for minimally invasive surgery with enhanced safety. *IEEE Robot Autom Lett (RA-L)* 4(3):2607–2613
25. Wang Z, Liu Z, Ma Q, Cheng A, Liu YH, Kim S, Deguet A, Reiter A, Kazanzides P, Taylor RH (2017) Vision-based calibration of dual RCM-based robot arms in human-robot collaborative minimally invasive surgery. *IEEE Robot Autom Lett (RA-L)* 3(2):672–679
26. O'Donnell CRD, Thomas Eggemeier F (1986) Workload assessment methodology. In: Boff KR, Kaufman L, Thomas JP (eds) *Handbook of perception and human performance. Cognitive processes and performance, vol II*. Wiley-interscience, New York, p 42-1–42-43
27. Hart SG, Staveland LE (1988) Development of NASA-TLX (Task Load Index): results of empirical and theoretical research. *Adv Psychol* 52:139–183
28. Yurko YY, Scerbo MW, Prabhu AS, Acker CE, Stefanidis D (2010) Higher mental workload is associated with poorer laparoscopic performance as measured by the NASA-TLX tool. *Simul Healthc* 5(5):267–271

Publisher's Note Springer Nature remains neutral with regard to jurisdictional claims in published maps and institutional affiliations.